

Reactive Halogen Chemistry in Volcanic Plumes

N. Bobrowski^(1), R. von Glasow⁽¹⁾, A. Aiuppa⁽²⁾, S. Inguaggiato⁽³⁾,*

I. Louban⁽¹⁾, O. W. Ibrahim,⁽¹⁾ U. Platt⁽¹⁾

(1) Institut für Umweltphysik, University of Heidelberg, Germany

(2) Dipartimento CFTA, Università di Palermo, Italy

(3) INGV – Sezione di Palermo, Italy

Abstract

Bromine monoxide (BrO) and sulphur dioxide (SO₂) abundances as a function of the distance from the source were measured by ground-based scattered-light Multi AXis Differential Optical Absorption Spectroscopy (MAX-DOAS) in the volcanic plumes of Mt. Etna on Sicily, Italy in August-October 2004 and May 2005 and Villarica in Chile in November 2004. BrO and SO₂ spatial distributions in a cross section of Mt. Etna's plume were also determined by Imaging DOAS. We observed an increase in the BrO/SO₂ ratio in the plume from below the detection limit near the vent to about 4.5×10^{-4} at 19 km (Mt. Etna) and to about 1.3×10^{-4} at 3 km (Villarica) distance, respectively. Additional attempts were undertaken to evaluate the compositions of individual vents on Mt. Etna. Furthermore, we detected the halogen species ClO and OCIO. This is the first time that OCIO could be detected in a volcanic plume. Using calculated thermodynamic equilibrium compositions as input data for a one-dimensional photochemical model, we could reproduce the observed BrO and SO₂ vertical columns in the plume and their ratio as function of distance from the volcano as well as vertical BrO and SO₂ profiles across

the plume with current knowledge of multiphase halogen chemistry, but only when we assumed the existence of an "effective source region", where volcanic volatiles and ambient air are mixed at about 600°C (in the proportions of 60% and 40%, respectively)

1. Introduction

The chemistry of volcanic plumes can give insights into volcanic processes, which could help to improve the forecast of volcanic eruptions [e.g., *Oppenheimer et al.*, 2003].

Volcanic plume chemistry is also of atmospheric relevance since volcanic aerosols and trace gases can have significant climatic impacts [e.g., *Robock*, 2000]. Despite their importance the chemical processes occurring in volcanic plumes are poorly understood. One reason for this is the difficulty of obtaining measurements of volcanic gas compositions.

Inorganic halogen species (X, X₂, XY, XO, HOX, XONO₂, HX, where X, Y = Cl, Br, I) have been known to be produced in the lower atmosphere either by degradation of organic halogen compounds or by oxidation of halides (X⁻) e.g. from sea salt [e.g., *Yvon and Butler*, 1996; *Finlayson-Pitts et al.*, 1989; *Platt and Hönninger*, 2003; *von Glasow and Crutzen*, 2003]. In this article we focus on a third potentially significant source of halogens to the atmosphere: volcanic emissions. BrO was detected in a volcanic plume for the first time at Soufriere Hills volcano on Montserrat [*Bobrowski et al.*, 2003], and has subsequently been measured at other volcanoes (a brief description of BrO levels and emissions of five different volcanoes can be found in *Bobrowski and Platt* [2006]). So far BrO has been detected at all volcanoes where the authors carried out measurements at distances exceeding about 1 km. Recently, ClO has also been detected in several volcanic plumes [*Lee et al.*, 2005; *Bobrowski*, 2005].

Gerlach [2004], based on theoretical considerations, argued that BrO is not a primary product of volcanic degassing, and suggested that its formation is due to high-

temperature oxidative reaction of magmatic gases with atmospheric components. More recently, *Martin et al.* [2006] presented more detailed equilibrium calculations for volcanic gas – air mixtures.

Here we present measurements of halogen oxides and SO₂ sampled at two different volcanoes, and discuss results from a one-dimensional numerical model simulating, for the first time, the temporal evolution and mechanisms of reactive halogen formation in volcanic plumes. By comparing field and model data, we test whether the measurements can be explained by known reaction mechanisms for the troposphere (for an overview see, e.g. *Platt and Hönniger* [2003] or *von Glasow and Crutzen* [2003]). Section 2 describes the instruments and locations where field data were acquired as well as the numerical model, the measurement results are discussed in section 3. The results of the model study are analyzed in section 4, which is followed by a concluding discussion in section 5.

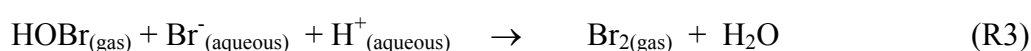
1.1 Chemical reactions in volcanic plumes.

In comparison to the background troposphere, very unique environmental conditions can be found in volcanic plumes. First, a huge number of solid and liquid particles is available (e.g., *Vie Le Sage* [1983]; *Mather et al.* [2003] and references therein), which provide a larger surface area for chemical reactions than normally found in the atmosphere. Second, besides other gases, high amounts of acids (HCl and H₂SO₄) are typically emitted or rapidly formed, which is reflected in the high acidity observed in the vicinity of volcanic vents [e.g., *Delmelle et al.*, 2003; *Allen et al.*, 2006]. The temperature in the initial plume is very high compared to ambient air, and because water vapour is, with carbon dioxide and sulphur species (SO₂ and H₂S), one of the main constituents of gaseous volcanic emissions [*Symonds et al.*, 1994], the initial humidity is also quite high compared to the background atmosphere.

As suggested by field studies and numerical simulations [Francis *et al.*, 1995, 1998; Gerlach, 2004; Aiuppa *et al.*, 2005], halogens are mainly emitted by volcanoes as hydrogen halides (e.g., HCl, HBr). Nevertheless, it has been shown by thermodynamic models that significant amounts of atomic halogen species (i.e., Cl, Br) can be produced by high-temperature oxidative dissociation in a volcanic gas-air mixture [Gerlach, 2004; Aiuppa *et al.*, 2005, Martin *et al.*, 2006], particularly above the so-called compositional discontinuity, at which drastic changes in the speciation of gases occur [Gerlach and Nordlie, 1975]. The subsequent dilution of the volcanic gas-air mixture with ambient air leads to the entrainment of O₃ and HO_x at the plume-edges promoting the onset of auto-catalytic radical reactions, including the oxidation of atomic species (XO, X = I, Br, Cl), in particular bromine:



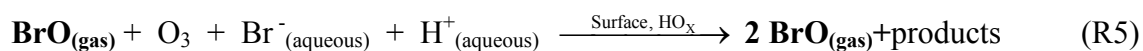
The presence of ozone and HO_x at the edges of the plume – mainly from entrainment and possibly from in situ formation of HO₂ under the high-temperature, high-humidity conditions in the early plume - leads to the rapid recycling of halogen oxides:



The required H⁺ (the reaction occurs at appreciable rates only at pH < 6.5 [Fickert *et al.*, 1999]) is supplied by strong acids, such as H₂SO₄, which are abundant in volcanic plumes (see above). The halogen molecule Br₂ is rapidly photolysed (at time scales on the order of minutes) to release the halogen atoms, which in turn react rapidly with O₃ (reaction R1); if ozone is available this will usually be the most likely process. Typical conversion time constants (O₃ ≈ 30 ppb) via R1 for e.g. X = Br are around 1 s. Bromine atoms are regenerated by photolysis of BrO:

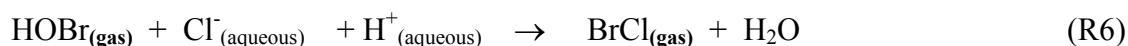


R4 in combination with reaction R1 leads to a photo-stationary state between Br and BrO with BrO/Br of the order of 10. In summary, reaction R3 followed by photolysis of Br₂, R1 and R4 promotes to a reaction cycle with the net result:

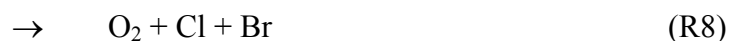


Effectively one BrO molecule is converted into two by oxidizing bromide at particle surfaces, of course at the expense of particle bromide. This process leads to an exponential growth of the concentration of gaseous BrO in the atmosphere (as long as there is ozone available), which gave birth to the term “bromine explosion” [Platt and Lehrer, 1997; Wennberg, 1999]. Using the term “bromine explosion” we refer to the non-linear increase in BrO concentrations similar to the auto-catalytic release mechanism of bromine from sea salt, which has been observed in polar regions.

In addition to bromine, Cl atoms (and ClO) could be produced via



followed by photolysis of BrCl and reaction R1. At high concentrations of BrO and ClO the following reactions take place:



OCIO and BrCl are readily photolysed to ClO and O, Br and Cl, respectively.

All above reaction mechanisms have been studied in detail in the laboratory and been found to be of importance in the tropospheric release of halogens from salts (see overviews of von Glasow and Crutzen [2003] and the compilations of Sander *et al.*

[2003] and *Atkinson et al.* [2004]). One of the goals of this study is to investigate if these reaction mechanisms can also reproduce the measured BrO, ClO and OCIO concentrations in volcanic plumes.

2 Methods and study area

2.1 The experimental set-up

At both Mt. Etna and Villarica Miniaturized Multi Axis Differential Optical Absorption Spectroscopy (Mini-MAX-DOAS) instruments were used to study the plume composition. The Mini-MAX-DOAS-system consists of an entrance optic (quartz lens with a focal length of 40 mm, and a lens diameter of 20 mm, field of view approximately 0.6°) coupled to a quartz fibre bundle, which transmits the light into a commercial miniature fibre optic spectrometer (OceanOptics Inc., USB2000) with a spectral resolution of 0.7 nm. This unit is placed inside an air tight metal housing and connected to a stepper motor gear combination, which can be mounted on a tripod. The stepper motor can turn the metal housing and therefore point the telescope at different elevation angles between 0° and 180° (from horizon to horizon, the telescope is pointed to the zenith in case of 90°). For a detailed description see *Bobrowski and Platt* [2006]. An UG5 filter blocks the visible light (wavelength > 400 nm) to reduce the stray light in the spectrometer. To prevent direct sun light from being scattered into the fibre and as a protection from acid rain a tubular black sun shield (22 mm diameter, 80 mm length) is attached in front of the entrance optics.

In order to reduce the dark current of the detector, a Charge Coupled Device (CCD), and to stabilize the optical bench the complete USB2000 spectrograph was cooled to a temperature of +10 °C during the measurements and for the measurements at the top of the volcanoes to 0 °C. Stabilizing the temperature of the spectrometer and detector readout electronics also reduced the temperature drift of the electronic offset signal. To

avoid water condensation the whole unit was made airtight and silica gel was added to keep the interior dry in case of leakage. The entire system (computer, cooling system, spectrometer and stepper motor) operates for several hours with a small lead acid battery (7.2 Ah) by using a handheld computer (Toshiba e400). Automatic data acquisition is performed by the special software package PocketDOAS [Lowe, 2004] running on a handheld computer. The complete measurement procedure, including the stepper motor drive changing the direction of view of the entrance optics, can be controlled by PocketDOAS.

The Imaging DOAS (IDOAS) instrument was used in May 2005 at Mt. Etna to investigate the spatial BrO/SO₂ distribution in the volcanic plume. IDOAS combines characteristics of the imaging spectroscopy, like spatial resolution, and the DOAS technique and therefore produces two-dimensional visualisations of trace gas distributions. The instrument used in this study utilizes an imaging spectrograph (Jobin – Yvon UFS200, f/# = 3.2) and a two-dimensional detector (ANDOR BU 420-BU, CCD, 255 vertical and 1024 horizontal pixels) to record spectral information from 280 nm to 380 nm of a solid angle of 0.09° width and 13.1° height. The instrument optics focuses light on the vertical entrance slit of the spectrograph, which images the slit on a column of the CCD detector (255 spatial pixel), whereas the light is spectrally resolved on a row (1024 spectral pixel) of the CCD detector. After the readout of the CCD, the spectral data of one vertical column with the solid angles (0.09° by 13.1° see above) is acquired. The instrument used in this study can cover a horizontal angle range of up to 70°. The horizontal resolution is given by the number of column scans and the azimuth angle between consecutive scans which is controlled by the scanning mirror. The vertical resolution is limited by the 255 pixels of the CCD detector. For a detailed description of the IDOAS [see Lohberger *et al.*, 2004; Bobrowski *et al.*, 2006; Louban, 2005].

2.2 Data Evaluation

The software WinDoas V2.10 from IASB (Belgium Institute for Space Aeronomy, [*Fayt and Van Roozendael, 2001*]) was used to derive the slant column densities (SCD) of BrO, ClO, OClO and SO₂ from the recorded spectra of both instruments.

As the light source is scattered sunlight, the solar Fraunhofer lines that modulate the radiation outside of the Earth's atmosphere have to be removed carefully in order to allow sensitive measurements of trace species. As Fraunhofer reference spectrum (FRS, $I_0(\lambda)$) a background spectrum after each plume scan was chosen and care was taken that the FRS did not contain absorption by the volcanic plume. To remove broadband structures as well as the effects of Rayleigh and Mie scattering a 2nd order polynomial was also fitted. For the evaluation of bromine monoxide a wavelength range containing 4 absorptions bands from 332 to 352 nm was chosen. Reference spectra of BrO, NO₂, O₃, SO₂, O₄, a 'Ring-spectrum' (to remove the effect of rotational Raman scattering in the atmosphere) and the FRS were simultaneously fitted to the measurement spectra using a nonlinear least squares method [*Stutz and Platt, 1996*], which is implemented in the evaluation software WinDoas (for further details see *Bobrowski [2005]* and *Bobrowski and Platt [2006]*).

The 'Ring effect' is caused by rotational Raman scattering [*Fish and Jones, 1995*] and leads to a reduction of the observed optical densities of solar Fraunhofer lines depending on the atmospheric light path.

The column densities of SO₂ and ClO were determined in the range from 306 to 315 nm, encompassing 3 ro-vibrational absorption bands of SO₂ and 2 of ClO. Besides SO₂ and ClO, a reference spectrum of O₃, a FRS and 'Ring-spectrum' as well as a 2nd order polynomial were included in the fit.

OClO was evaluated in the range from 362 nm to 390 nm and 341 nm to 390 nm, with 3 and 6 absorption bands, respectively. Reference spectra of OClO, BrO, NO₂, O₃, SO₂, O₄, a 'Ring-spectrum' and the FRS were simultaneously fitted as well as a polynomial of

third and fifth order, respectively. Both evaluations lead to the same result (within a 2σ error).

2.3 Model description and setup

The one-dimensional model MISTRA [von Glasow *et al.*, 2002] was used to simulate the evolution of an air column that has been influenced by volcanic emissions. We compare the model results with observed column densities of BrO, ClO, OClO, and SO₂ in order to test if our current knowledge of atmospheric multi-phase halogen chemistry is sufficient to simulate the observations in volcanic plumes. The model describes in detail the chemical processes occurring in the gas and aerosol phase. In the microphysical part of the model the growth of the particles as well as the interaction of microphysics with radiation is considered, however, the current model version does not include aerosol collision/coalescence or new particle formation. The chemical mechanism focuses on halogens; it has been updated from von Glasow and Crutzen [2004] according to Sander *et al.* [2003] and Atkinson *et al.* [2004] and includes 170 reactions in the gas phase (including photolysis) and 265 in the aqueous phase (including equilibria and heterogeneous reactions).

The basic setup of the model runs is that a column of air is moving over a volcano where the plume is emitted as a puff into three adjacent model layers at about 3340m. This column of air is then advected downwind according to the model wind speed of 10 m s⁻¹. We ignore any local effects of the mountain orography on the flow and account for increased turbulence by adjusting our entrainment parameters (see below). Tests have shown that the vertical model layer depth Δz should not be greater than 10m in order to avoid unrealistic stepwise entrainment of unpolluted air from above when the plume expands to the next higher model layer. This effect is strongly reduced with $\Delta z=10\text{m}$,

compared to $\Delta z=15\text{m}$ or 20m , though still occurring as evident as spikes in the BrO vertical column (see Figure 11, especially case “pure”).

Vertical dilution of the plume is calculated explicitly with the standard turbulent diffusion routine in the model [Mellor and Yamada, 1982], while horizontal dilution is taken into account with a simple parameterization, assuming that the horizontal evolution of the plume corresponds to a Gaussian plume (see e.g. Seinfeld and Pandis [1998]). Close to the source the horizontal plume width is proportional to the time elapsed since plume emission, at greater distance it is proportional to the square root of the time. Note, that by using this approach we assume the expanding plume to be well mixed horizontally up to the width of the Gaussian plume. The composition of the entrained background air is taken from a second model run with the same initialization but without emission of a volcanic plume.

Our tests have shown that the values obtained for the plume width calculated after Seinfeld and Pandis [1998] (equations 18.22, 18.24, 18.25) drastically overestimate the stability of the plume, probably because the empirical parameters were derived for plume release close to the ground. Therefore we artificially increased the dilution by specifying a minimum entrainment coefficient based on a comparison of measured SCD and modelled vertical columns of SO_2 .

Next to the dilution of the plume with background air the specification of the composition of the initial plume is crucial. We calculated the composition of the fresh plume (plume in the uppermost part of the vent) with the commercial software HSC (Outokumpu Tech., Finland), assuming thermodynamic equilibrium within the volcanic gas – air system. The fact that high temperature volcanic gases are equilibrium systems at pressure – temperature – oxygen fugacity (P-T-f O_2) conditions of the melt has long been recognised [Gerlach and Nordlie, 1975]. In line with recent modelling efforts satisfactorily using the same HSC software [Gerlach, 2004; Martin et al., 2006], we assume the gases to be in

equilibrium also in the case of high temperature air-volcanic gas mixtures, particularly when reaction kinetics proceed faster than air-dilution itself which we assume to be the case for $T \geq 600$ °C. The HSC software uses a free-energy minimization algorithm in order to calculate the molecular equilibrium composition of a gas mixture, given its starting elemental composition, T and p. We show model runs for different initial elemental compositions formed by variable mixtures of volcanic gases and ambient air, where Etna's volcanic gas composition (H_2O , 78%; CO_2 , 8.7%; SO_2 , 2.6%; HCl, 1.3%; HBr, 0.006 %) is from *Aiuppa et al.* [2005] and additional calculations with HSC. Furthermore, we compare model runs based on this data with a run based on the numbers from *Gerlach* [2004] for mean compositions of arc volcanoes at 900°C (“arc mean”) with a mixture of 85% plume air and 15% background air for several types of volcanoes. As Mt. Etna is not an arc volcano; we use the data from *Gerlach* [2004] not to compare them to field data but to show the differences in the plume evolution in the model for different types of volcanoes. The initial composition of the aerosol is taken from *Allen et al.* [2006], whereas the aerosol size distribution is taken from *Watson and Oppenheimer* [2000].

The operator splitting time step for aerosol microphysics, transport, and chemistry is 10 s. Within these 10 s, the set of chemical equations is solved with an automatically adjusted sub-time step with a Rosenbrock solver. To avoid numerical instabilities we include an equilibration step for aerosol and gas phase after the plume dilution has been calculated in each time step. The model runs start at local noon, the plume is emitted into free tropospheric air 11 minutes after model start. Note, that only the first approximately 30 - 60 minutes of the plume evolution in the model is covered by the measurements. The comparison of model results with volcanic data is difficult as data even from the same campaign has usually been sampled at different locations and/or different times. The system is expected to have, and many measurements show that, a strong day-to-day,

campaign-to campaign, volcano-to-volcano variability. However, for halogen oxides and aerosol often only single data points are available. Many of the reactive gas data only refer to the total column but do not include variations across the plume, hardly any in-situ data of gases in the plume are available. The initial plume composition is derived from thermodynamical equilibrium calculations for “typical” Etna conditions as explained above but one might expect them to vary during different stages of volcanic activity. In summary, no exact fit of field data and model results can be expected; therefore we present only qualitative and semi-quantitative comparisons.

2.4 Measurement locations

Mt. Etna

Mt. Etna is situated on Sicily, an island to the south of Italy in the Mediterranean Sea (37.73° N, 15.00° E). Mt. Etna, one of the largest and most active continental volcanoes in the world, started its activity about 0.6 Ma ago [Bonaccorso *et al.*, 2004]. The base of the volcano is about 60km by 40km and its summit reaches 3340 m above the sea level. Below an elevation of about 2900m Etna has the typical shape of a shield volcano. It is adorned with more than 200 craters on its slopes. Much of the volcano's surface is covered by historic lava flows, mostly hawaiitic in composition (e.g., SiO₂, 45-52 wt. %; Na₂O-K₂O, 5-7 wt. %). The mountain shows eruptive as well as quiescent activities. During 2001 and 2002-2003, two large flank eruptions took place [Andronico *et al.*, 2005; Behncke and Neri, 2003]; since February 2003, the activity of Etna has taken the form of persistent quiescent degassing occurring from the four active summit craters (Bocca Nuova (BN), Voragine (VOR), Southeast (SE) and Northeast (NE), see also Figure 6.1). More recently, on September 7, 2004, a new effusion event on Etna's eastern flank started, which stopped on March 13, 2005 [Burton *et al.*, 2005]. This eruption fell partly into the measurement period.

In August 2004 DOAS data were collected from Pizzi Deneri (Fig. 2, point c), on Etna's NE upper flank. In azimuthal direction the telescope pointed about 3 km downwind from the summit while the telescope elevation angles were increased from 15° to 55° in steps of 5°, continuing with 80°, 100° and 110°. During September-October 2004 measurements at different sites were carried out as marked by red dots in Figure 1. The telescope elevation angles were chosen depending on the observation site and the direction of the plume. Most of the observations took place on the eastern flank of Mt. Etna at Rifugio Citelli (Figure 1 d), 6 km downwind of the summit.

On October 1, 2004 an attempt was made to scan plumes originating from different summit vents, before they were mixed to investigate possible differences in emission characteristics.

In May 2005 three Mini-MAX-DOAS instruments were operated, allowing the simultaneous determination of the plume BrO/SO₂ ratio from three different locations (at increasing distances from the summit area). Additionally, measurements were carried out with the IDOAS instruments on several days, however only the data of May 10, 2005 are considered here. On May 9 2005, a very sunny day, simultaneous Mini-MAX-DOAS measurements at 6, 10 and 19 km took place on the eastern flank of Mt. Etna (Figure 1 red triangles). Every day measurements were carried out at Rifugio Citelli, to investigate short-term temporal variations of BrO/SO₂ ratios inside the volcanic plume. The plume was scanned with telescope elevation angles ranging from 0° up to a maximum of 130° in usually 5° to 10° steps depending on the actual plume-shape at the time.

Insert Figure 1

Villarica

Villarica is situated in the southern Andes in Chile (39.3° S, 71.4° W). It is a basaltic-andesitic open-vent stratovolcano with a height of 2847 m above sea level and with a long historic record that includes fatal eruptions [Witter *et al.*, 2004]. A very large

(Volcanic Eruption Index VEI = 5) eruption was dated at ca. 1810 B.C. by using the radiocarbon method. The first historic eruption was recorded in 1558. Since then numerous small gas explosions occurred throwing incandescent blobs of lava above the crater rim. Larger eruptions and lava flows were less frequent. Since the end of the last eruption in 1985 an active lava lake has been present in the summit crater and the volcano has been continuously degassing [Moreno *et al.*, 1994].

Measurements at Villarica volcano were performed on November 17, 2004 (Figure 1 Villarica point (b)) and November 24, 2004 (Figure 1 Villarica point (a)). On November 17, 2004 the MAX-DOAS instrument was pointed about 3 km downwind of the summit of the volcano and the plume was scanned at telescope elevation angles 1°, 24°, 27°, 30°, 33°, 36°, 39°, 50°, 60°, 70°, 90° above the horizon. On November 24, 2004 an expedition to the top of the volcano was successfully carried out and measurements near the crater rim took place for 1 hour. A white cloud layer could be seen below the measurement site and a puffing plume was observed, probably caused by intermittent lava spattering inside the main degassing vent. The plume was scanned from 5° to 29° with steps of 3° above the horizon; two spectra at 90° and 150° (away from the plume) were taken.

3) Results and discussion

3.1. Investigation of spatial BrO distribution in volcanic plumes

In tropospheric volcanic plumes, the loss of sulphur dioxide via reaction with OH and/or uptake into particles is slow, at least in the early plume stages and under ash-free conditions [e.g., McGonigle *et al.* 2004]. Therefore, the evolution of SO₂ concentration is dominated by dilution, and the ratio of other species to SO₂ enables us to separate changes caused by chemical processes and dilution. In order to investigate the chemical evolution of BrO with time in the plume, we measured at different distances from the

crater and calculated the ratio of BrO to SO₂. However, simultaneous measurements at different distances are available only for the campaign in May 2005.

Insert Figure 2 and 3

Figures 2 and Figure 3 show examples of individual plume scans of typical BrO and SO₂ SCDs at Mt. Etna and Villarica, respectively. During the field campaigns of August – October 2004, data for different distances ((a) several 100s of metres, (b) 1.5km, (c) 3km, (d) 6km, and (e) 19km) could not be collected simultaneously as only two instruments were available. No BrO ($> 4 \times 10^{13}$ molecules/cm²) could be detected in the “near-vent” plume of the Voragine crater at Mt. Etna (see Figure 2 a). At a distance of 1.5 km (Figure 2.b), which corresponds to a plume age of about 300 s (assuming a wind velocity of 5m/s), BrO can already be clearly detected in the plume. Due to the dispersion of the plume, the SCDs decrease significantly as the plume propagates downwind, which leads to higher relative errors further downwind for BrO as well as for SO₂ (Figure 2e). The ratios of BrO to SO₂ at several distances from the crater are shown as dotted bars in Figure 4; they increase with distance from the crater. As the 2004 measurements for different distances were not taken on the same day, one might argue that the variations in BrO/SO₂ may be caused by differences in volcanic activity, rather than by chemical processes in the plume. On May 9 2005, however, we repeated the experiment by measuring simultaneously at three distances from the summit region of Mt. Etna (6km, 10km, 19km) and found the same pattern, namely an increase of the BrO to SO₂ ratio with distance and therefore with chemical processing time within the plume (see Figure 2 and 4 - red solid bars).

Insert Figure 4

Assuming, as mentioned above, that the $[\text{SO}_2]$ changes in the first kilometres of a volcanic plume are only due to dilution but not chemistry (see *McGonigle et al.* [2004] and our model results) the change in the BrO to SO_2 ratio has to be caused by BrO production in the plume. This is plausible and supported by our model runs and is also consistent with the findings of *Oppenheimer et al.* [2006]. The same conclusion can be drawn for the data collected at the volcano Villarica, see Figure 3 and 4 (blue, solid bars).

In May 2005 additional measurements were carried out with the IDOAS instrument with the aim to investigate the spatial distribution of BrO and SO_2 in the plume of Mt. Etna in detail. In order to improve the current BrO detection limit for the IDOAS, measurements with the viewing direction along and not perpendicular to the plume were undertaken on the May 10, 2004, thus increasing the light paths inside the plume.

Figure 5 shows one vertical plume profile of the BrO/ SO_2 ratio, calculated from the simultaneously measured two-dimensional BrO and SO_2 distributions within the plume. In this case BrO SCDs of each IDOAS-image row were outlined against the SO_2 SCD values of the same IDOAS-image row. A linear fitting procedure gains the gradient, which is the BrO/ SO_2 ratio in this part of the investigated plume and the correlation coefficient R. Due to the higher spatial resolution ($0.1^\circ \times 0.26^\circ$) compared with the Mini-MAX-DOAS measurements, the structure of the BrO/ SO_2 ratio inside the plume is revealed. BrO, in comparison to SO_2 , is enhanced at the edges of the plume, which can be explained by increased entrainment of O_3 -rich ambient air into the volcanic plume margins. This effect is also present in our model calculations (see below).

We are aware that the relative error of the BrO SCDs at the plume edges is increased due to the shorter light paths inside the volcanic plume. Nevertheless, even considering these higher errors (which are included in the calculation for the error bars in Figure 5) the increasing trend of the BrO/ SO_2 ratio is still visible.

Insert Figure 5

Due to favourable conditions on October 1, 2004 (it was a very clear day and the clouds which appeared around midday were below the measurement site), we investigated the composition of plumes released by individual craters of Etna. As can be seen from Figure 6.1 the measurement site (red triangle) is located in between the plumes from the NE and the VOR craters. We made a scan through both plumes by aiming perpendicular to the plume axis and scanning from a telescope elevation angle of 15° to 160° , therefore first probing the plume from the NE crater and then the one from the VOR crater (see Figure 6.1). This shows a higher BrO/SO₂ ratio to the northeast of the measurement site (telescope elevation angles $15^\circ - 70^\circ$ on Figure 6.2), dominated by the NE crater plume than to the southwest (telescope elevation angles $90^\circ - 140^\circ$) dominated by the VOR and BN crater plumes.

Insert Figure 6

These observations suggest an enrichment of halogens at the NE crater (or a depletion of SO₂) in comparison with the Voragine crater and Bocca Nova; this is also supported by routine filter pack measurements carried out over 2004 [Aiuppa *et al.* 2005].

3.2. Investigation of temporal variations in the BrO/SO₂ ratio

Further observations were made in order to investigate not only the spatial variation of the BrO/SO₂ ratio, but also the temporal variations of the BrO/SO₂ ratios. To achieve this, measurements from one fixed position (Rifugio Citelli about 6 km downwind the summit; Figure 1 red dot and triangle (d)) were carried out during both field-campaigns (2004 and 2005). This location was chosen due to the favoured westerly winds at Mt. Etna and the consequential higher possibility of plume overpasses over this area.

The BrO/SO₂ ratio appears to be quite stable during mid October and slightly higher than in September (see Figure 7.1). Results of May 2005 measurements are more scattered than those from September-October 2004 field campaign. The BrO/SO₂ average from 2005 value exceeds those from 2004. The weather during both time series changed from very sunny to very cloudy including some rain events and can be considered as similar for both periods. No exceptional activity at Mt. Etna was recorded in May 2005 (see for further information the weekly reports of Catania: www.ingv.ca.it). An explanation for the larger scatter of the BrO/SO₂ ratios in May 2005 could be found in the greater variability in the wind direction (see Figure 7.2), possibly resulting in varying influence of the NE and Voragine crater, which have significantly different BrO/SO₂ (see Figure 6.2). From Rifugio Citelli often only part of the plume could be measured and it is likely that at a distance of 6 km the plumes of the NE and Voragine craters are still not completely mixed so that the observed difference in the BrO/SO₂ ratio is indeed caused by the different crater plumes. The wind data suggest that it is possible that the plume of the NE crater influenced the May 2005 measurements more than the measurements carried out in September and October 2004. As shown above and by *Aiuppa et al.* [2005], the NE crater is - relative to SO₂ - richer in halogen compounds than, for instance, Voragine.

Insert Figure 7

3.3. Detection of OCIO and ClO

August 5, 2004 was very clear in the morning and measurements were made at Pizzi Deneri 3 km downwind from the crater (site c in Figure 1). The plume was studied under several telescope elevation angles and trace gas SCDs were quite high as the plume was relatively narrow. One plume scan from this day is taken as an example to present the data for OCIO and ClO, in addition to BrO and SO₂ (Figure 8). The SCDs of these four

species are plotted as a function of the telescope elevation angle and error bars for 1 sigma error resulting from the DOAS-fit, a nonlinear least-square fit (Levenberg-Marquard), are shown for each data point. Peak SCD's of OCIO and ClO reached 2.45×10^{14} and 2.1×10^{17} molecules/cm², respectively. Both chlorine oxides correlate well with BrO and SO₂ in the plume (see Figure 8). The OCIO/SO₂ ratio is 5.7×10^{-5} , which is about one quarter of the BrO/SO₂ ratio, which in this case is 2.1×10^{-4} . ClO is about 20 times less abundant in the plume than SO₂ but there are some problems with the ClO evaluation [Bobrowski, 2005]. Strong absorption bands of ClO are located at ≤ 308 nm. At these wavelengths the solar intensity is quite low (due to O₃ absorption), thus the photon shot noise - already a limiting factor for a good quality evaluation - is relatively high. The other problem is the possible interference of absorption of other trace gases in this wavelength region. Several evaluation settings were investigated. They clearly showed that care has to be taken when deriving informations on the ClO abundance in volcanic plumes with scattered - sunlight DOAS. Only data from very sunny days should be used. Further research and improvements are necessary in the future, like an improved Ring spectrum.

Due to these experimental problems it is very valuable to have further indications for the presence of chlorine oxides. OCIO is produced in the reaction of ClO with BrO (R7) and therefore a good indication for the presence of ClO. During this study OCIO was detected in the troposphere for the first time. Therefore an example of a fitting result (the optical density of the OCIO absorption as a function of wavelength) from the centre of the plume is shown in Figure 9. Since the absorption structures of OCIO are located at longer wavelengths its detection is much more reliable than that of ClO.

Insert Figure 8

Insert Figure 9

4. Model results and discussion

Simulations with the model introduced in section 2.3 show that we can reproduce the measured columns of BrO and SO₂ much better when we specify the composition of the initial plume according to the results of a thermodynamic equilibrium speciation model for a mixture of volcanic gases and ambient air, rather than pure volcanic gases. Such a mixture results in a plume with higher oxygen content but lower temperature than for a case with “pure” volcanic volatiles, leading to a modified speciation which especially increases the concentration of dihalogens and reduces SO₂. *Gerlach and Nordlie [1975]* were the first to describe the so-called compositional discontinuity, which leads to a drastic change in the speciation at a certain ratio of ambient air to volcanic volatiles. A higher fraction of ambient air additionally implies smaller temperatures of the gas mixture (e.g., 600°C instead of 1100°C for pure volcanic volatiles) which again leads to changes in the speciation of the gas mixture. We refer to the part of the crater where the very first interactions between the volcanic volatiles and ambient air occur, leading to these distinct changes in the plume composition, as the “effective source region”. This region is shown schematically in Figure 12.

In the following, we discuss model runs with four sets of different initial compositions of the plume based on thermodynamic equilibrium speciation models (see Table 1 for the initial gas phase composition of four different model runs) All runs include aerosol phase chemistry, as runs that do not take aerosol chemistry into account showed that the observations, especially the BrO levels, could not be reproduced. The results that compare best with measurements from Mt. Etna are from a run with a mixture of 60% volcanic gases and 40% ambient air at 600°C (this run is abbreviated with “60-40”). Furthermore, we show results from a run with an initial composition of 85% volcanic air and 15% ambient air at T=900°C (“85-15”) and pure volcanic gases at 1100°C (“pure”). These three runs are for Mt. Etna magmatic gas composition, whereas the initial

conditions for the fourth run are taken from *Gerlach* [2004], for mean compositions of arc volcanoes at 900°C (“arc mean”). As mentioned above, the latter case is not appropriate for a comparison with data from Mt. Etna; we show it to highlight the possible range of halogen chemistry in volcanic plumes in general.

Figure 10 shows the results for case “60-40” as a function of altitude and time since model start. Directly after plume release all ozone is titrated by NO, the latter being a by-product of high-temperature air-volcanic gas reactions [*Martin et al.*, 2006]. Due to the temperature difference between the plume and ambient air the plume rises, increasing the entrainment of O₃-enriched air from above. The speciation of the bromine compounds in the plume depends on the initial NO_x content of the plume (or more precisely: the formation of NO_x in the effective source region): in cases “85-15” and “arc mean” the resulting NO₂ reacts with Br producing BrNO₂ whereas in case “60-40” the NO_x concentrations are high enough to titrate all O₃ but not high enough to make BrNO₂ the main reservoir of bromine, in this case most bromine exists as Br-atoms. During this time, BrO in the model is only formed at the upper and lower plume edges because the ozone concentrations are close to zero in the core of the early plume. In all discussed model runs dilution with background air leads 10-20 minutes after plume release to a strong decrease in the concentrations of all species that had been emitted or produced in the effective source region and to a replenishment of O₃, which then reacts with Br to produce BrO. In the model this leads to a gradual build-up of BrO (see Figure 10) that has also been observed in the measurements (see Figures 3-5). The high BrO mixing ratios are sustained above the pmol mol⁻¹ level in the model for about 3 hours by the heterogeneous “bromine explosion” recycling mechanism described in the introduction until dilution of the plume by entrainment of background air becomes too strong. The scenario “pure” is distinctly different from the others, as here very little NO_x is “emitted”. BrO formation at the upper and lower plume edges starts earlier than in the other runs.

These comparisons show that differences between the various scenarios are mainly caused by different levels of NO_x and the speciation of halogens which is a strong function of temperature and the fraction of ambient air in the effective source region. We calculated the vertical column densities of BrO, SO_2 , OClO, and ClO from the model (see Figure 11) for comparison with the field-measured slant column densities. Note that the spikes in the BrO vertical columns are caused by the vertical expansion of the plume into the next higher level (see Section 2.3), therefore starting the “bromine explosion” mechanism in each model level where plume air is mixed with ambient air containing O_3 . These spikes are model artefacts which would only be avoidable with an even higher vertical resolution, however they do not affect the overall model results but highlight the importance of the “bromine explosion” mechanism. The magnitude of the modelled BrO columns are very similar to the measured values and differ little between the different scenarios even though the amount of gas phase bromine (including HBr) that the model was initialized with varies by 3 orders of magnitude among the different runs, showing that cycling between the gas and aqueous phases and the entrainment of O_3 are the key processes in determining BrO. The evolution with time is different for each scenario, case “pure” being the one that compares least well with the measurements as its BrO vertical column stays approximately constant with time. The other three runs show a gradual rise of BrO caused by the “bromine explosion” mechanism. The different timing is a consequence of the different initial compositions of the plume resulting in earlier or later “ignition” of the “bromine explosion” in each case.

The calculated SO_2 columns also compare well with the measurements. They are mainly determined by dilution as gas phase oxidation via OH is negligible due to very small concentrations of O_3 and therefore OH in the plume, all other gas phase loss reactions of SO_2 are too slow under atmospheric temperatures [see *Sander et al.*, 2003 and *Atkinson et al.*, 2004]. Uptake of SO_2 to the particles is limited due to the very low aerosol pH.

These results and the discussion earlier in this article indicate that SO₂ can be regarded as quasi-passive tracer, so that the use of ratios like BrO/SO₂ will help us to understand bromine photochemistry in the plume. The initial SO₂ concentration is a strong function of plume composition and case “60-40” compares best with the measurements but its dilution still seems to be somewhat delayed compared to measurements.

All runs show a gradual rise in the BrO/SO₂ ratios (see Figure 11a, b), the temporal evolution being determined both by the initial SO₂ concentration and the photochemical evolution of BrO. Again case “60-40” shows the best agreement with the measurements, matching the measured numbers well (see Figure 11a vs. 4; note that the plume is emitted 11 minutes after model start). The model also reproduces the IDOAS measurements, showing that the BrO/SO₂ ratio has a maximum at the upper and lower plume edges (see Figures 6 and 10, note that the IDOAS measurements were made within the first 30 minutes after plume release). According to the model, the BrO columns stay fairly constant for some time (see Figures 11a, b). As already explained, the SO₂ concentrations are mainly determined by dilution so that the BrO/SO₂ ratio keeps increasing for about 2-3 hours after plume release until dilution has decreased the concentrations of all compounds in the plume strongly (see Figure 11b). According to the horizontal dispersion parameterization that we are using, the plume width is about 15km three hours after plume release. During this time, the bromine speciation in the model also changes drastically. In the first hour after plume release gas phase bromine is largely in the form of Br, then BrO becomes the main bromine-species and eventually, at the same time as the BrO/SO₂ ratio starts decreasing, most gas phase bromine is present as BrCl. HBr is never a dominant gas phase bromine reservoir as it is rapidly taken up by particles and re-released as Br₂ or BrCl to the gas phase, except probably in the near-vent plume. The shifts in the bromine speciation are caused by the varying O₃ concentrations and the non-linearity's in the chemical system, for example caused by the BrO self

reaction. These model predictions – the continued rise in the BrO vertical column and the shape of the BrO/SO₂ ratio as function of distance/time from the plume - should be tested in future field campaigns.

The initial plume composition as well as the entrainment rate are the main factors in determining the temporal evolution of the BrO vertical columns in the model and the ratio of the BrO/SO₂ columns. Overall, the comparison of the ratio of the BrO and SO₂ columns show very good agreement with the measurements, especially when taking into account the uncertainties of the composition of the initial plume and the simplicity of our mixing approach.

The comparison of the column densities of ClO and OClO between model and measurements, however, shows a very large underestimation by the model of up to 4 orders of magnitude. Only in case “60-40” the mismatch is reduced for ClO to a factor of about 30 (in Figure 11a the ClO vertical columns are depicted with different scaling to show the differences between the four model scenarios). Since ClO is the precursor for OClO (via self-reaction and reaction with BrO), we cannot expect to obtain realistic OClO levels in the model without first having realistic ClO values. In order to facilitate the following discussion we define the sum of all gas phase chlorine as Cl_{tot} and Cl_x=Cl_{tot} – HCl, and Br_{tot} and Br_x accordingly. The release of Cl_x is highest in case “60-40” and is the reason why here initially high ClO vertical columns are present in the model. The release of Cl_{tot} is similar in the different model scenarios. In contrast to HCl, HBr is rapidly taken up by particles resulting in a small difference between Br_{tot} and Br_x, whereas the opposite is true for Cl_{tot} and Cl_x. For bromine this means that in the model most bromine is rapidly recycled between the gas and aerosol phase. Chlorine, however, remains largely in the gas phase in the less reactive form of HCl and is only taken up in a minor fraction as particulate Cl⁻. This difference between chlorine and bromine is mainly caused by the different acidity constants for HCl and HBr and the very low particle pH.

This points to a possible explanation for the large mismatch between model and field results for ClO: the lack of efficient recycling mechanisms in the model that convert HCl/Cl⁻ into more reactive chlorine at low pH. Another possibility is an erroneous initial plume composition in the model. Additional tests showed that assuming even higher fractions of ambient air in the “effective source region” for the plume would not improve the results. If the model prediction of an almost O₃-void plume is correct, the early-plume ClO and OClO signals in the MAX-DOAS observations would either have to come from the edges of the plume only, as O₃ is the main prerequisite for both BrO and ClO formation or some chlorine-specific inter-conversion reactions among different chlorine oxides could be occurring in the plume. These options and further model scenarios will be explored in a forthcoming publication (*von Glasow, in preparation*).

5. Conclusion

This study is a first detailed account of the potential photochemical processes occurring in quiescently degassing volcanic plumes, highlighting the potential importance of volcanoes for tropospheric photochemical processes. The measurements of the slant column densities of BrO and SO₂ in volcanic plumes at two volcanic sites (Etna in Southern Italy and Villarica in Chile) and their comparison with a numerical model suggest that BrO is formed by heterogeneous photochemistry downwind of the crater. The comparison with first model studies are qualitatively and semi-quantitatively in good agreement, provided that the initial plume composition corresponds to a high-T (600°C) volcanic gas-ambient air mixture (in the proportions of 60% and 40%, respectively). The increase in BrO in our model is caused by the entrainment of O₃ rich air into the previously O₃-free plume and the subsequent start of the “bromine explosion” mechanism. This is consistent with the experimental finding that both the BrO vertical columns and the BrO/SO₂ ratio increase with time and that BrO is not uniformly distributed over the plume cross section, but rather shows maxima at the plume edges,

where entrainment of O₃-rich air is highest. The chlorine oxides ClO and for the first time OCIO were detected as well in the plume of Mt. Etna. Both species are, however, dramatically underestimated by the model, pointing to some unaccounted for chemistry and/or an initial plume composition that varies from that which we calculated using a thermodynamic-equilibrium speciation model.

In summary, our comparison of field observations with an atmospheric photochemical model initialized using the results from a thermodynamic equilibrium model, suggests that the processes in the plume occur in the following steps (see Figure 12):

- 1) Degassing of hot (~1100°C) volcanic gases from the silicate melt. Due to the high temperatures, gas-phase equilibrium at the melt T-P-fO₂ conditions can be assumed [Symonds *et al.*, 1994], and the composition of the volcanic gas phase is likely to be a mixture of H₂O, CO₂ and SO₂ – plus minor gaseous hydrogen halides (HCl and HBr) and particles – in the proportions given by Aiuppa *et al.* [2005]. Immediately after emission a mixture of volcanic volatiles and ambient air (the “volcanic plume”) with still high temperatures (~600°C) forms. According to the thermodynamic equilibrium model, the resulting high oxygen concentration in this gas mixture in comparison to the pure volcanic gas case leads to dramatic changes in halogen and nitrogen speciation. These changes have already been described for other compounds by Gerlach and Nordlie [1975] as “compositional discontinuity” and provide reactive precursors for the following photochemical processes in the atmosphere (especially for halogens and NO_x). We refer to the region in the crater where the initial mixing of volcanic volatiles with ambient air occurs under high temperatures as the “effective source region”
- 2) Subsequently, further mixing with ambient air rapidly cools the plume (within several minutes) to temperatures close to ambient conditions and water vapour condenses onto particles. Ozone is entrained with the ambient air at the plume

edges, starting radical chemistry. Hydrogen halides (in particular HBr) dissolve in the liquid layer of the particles.

- 3) Once OH and HO₂ radicals are available, the specific conditions in the plume (large specific surface area, acidity, humidity) lead to the autocatalytic release of reactive halogen species (BrO, ClO) from the halides (“bromine explosion”) due to rapid cycling between the gas and aqueous phase.

The model results suggest that the BrO levels remain high for about 2-3 hours after plume release and that the BrO/SO₂ keeps increasing during this time. This finding should be tested in upcoming field campaigns. More data on chlorine compounds in the plume, especially their temporal evolution, are needed in order to improve our understanding of chlorine chemistry in the plume. To facilitate the assessment of the influence of the emissions of slowly degassing volcanoes on atmospheric chemistry, measurements further downwind in the plume and not only in the first 10-20 km are needed.

Acknowledgements

We thank the people of INGV in Palermo and Catania for their support on Italian Volcanoes, particularly Salvatore Giammanco, Manuela Bagnato, Dimitri Rouwet, Roberto Inguaggiato. We also thank all other participants of the measurement campaigns, especially Nuccio Faro, Andrew McGonigle, Tamsin Mather, David Pyle, Andrew Allen, Bo Galle, John Murphy, Jose Ignazio, Carlos Jose Ramirez, Bill Morrow, Nick Varley. Without the huge amount of help, financial and logistical support for the sites this kind of measurements would not have been possible. We thank Greg Lowe for the development of the Pocket-DOAS software. We want to thank Tamsin Mather, Alfonso Saiz-Lopez, Christiane Textor and Terrence Gerlach for valuable comments on the manuscript.

Financial support by the European Union through the project DORSIVA is gratefully acknowledged. RvG is funded by the German Deutsche Forschungsgemeinschaft (GL 353-1/1,2).

References

- Aiuppa, A., C. Federico, A. Franco, G. Giudice, S. Guirriere, S. Inguaggiato, M. Liuzzo, A.J.S. McGonigle and M. Valenza (2005), Emission of Trace Halogens From a Basaltic Volcano: Mt. Etna., *Geochem. Geophys. Geosys.* (6), doi:10.1029/2005GC000965.
- Allen, A. G., T. A. Mather, A. J. S. McGonigle, A. Aiuppa, P. Delmelle, B. Davison, N. Bobrowski, C. Oppenheimer, D. M Pyle, and S. Inguaggiato (2006), Sources, size distribution, and downwind grounding of aerosols from Mount Etna, *J. Geophys. Res.*, *111*, (D10302), doi:10.1029/2005JD006015.
- Andronico D., Branca S., Calvari S., Burton M.R., Caltabiano T., Corsaro R.A., Del Carlo P., Garfi G., Lodato L., Miraglia L., Muré F., Neri M., Pecora E., Pompilio M., Salerno G., and L. Spampinato (2005), A multi-disciplinary study of the 2002-03 Etna eruption: insights for into a complex plumbing system. *Bulletin of Volcanology*, 10.1007/s00445-004-0372-8
- Atkinson, R. and D. L. Baulch and R. A. Cox and J. N. Crowley and R. F. Hampson and M. E. Jenkin and J. A. Kerr and M. J. Rossi and J. Troe (2004), Summary of Evaluated Kinetic and Photochemical Data for Atmospheric Chemistry, Web Version, July., <http://www.iupac-kinetic.ch.cam.ac.uk>
- Behncke, B., and M. Neri (2003), The July – August 2001 eruption of Mt Etna (Sicily), *Bull. Volcanol.*, *65*, 461– 476.

- Bobrowski, N., Hönninger, G., Galle, B. and U. Platt (2003), Detection of Bromine Monoxide in a Volcanic Plume, *Nature*, 423, 273-276.
- Bobrowski, N. (2005), Volcanic Gas Studies by Multi Axis Differential Optical Absorption Spectroscopy, *PhD thesis*, Institut für Umweltphysik, Universität Heidelberg.
- Bobrowski, N., and U. Platt (2006), Bromine Monoxide Studies in Volcanic Plumes, *J. Volc. and Geotherm. Res.*, In review.
- Bobrowski N., Hönninger G., Lohberger F., and U. Platt (2006), IDOAS: A new monitoring technique to study the 2D distribution of volcanic gas emissions, *J. Volcanology and Geothermal Res.*, 150, 329-338.
- Bonaccorso, A., S. Calvari, M. Coltelli, C. Del Negro, and S. Falsaperla (2004), Mt. Etna: Volcano Laboratory, *Geophysical Monograph 143*, American Geophysical Union.
- Burton, M.R., M. Neri, D. Andronico, S. Branca, T. Caltabiano, S. Calvari, R.A. Corsaro, P. Del Carlo, G. Lanzafame, L. Lodato, L. Miraglia, G. Salerno, and L. Spampinato (2005), Etna 2004-2005: An archetype for geodynamically-controlled effusive eruptions, *Geophys. Res. Lett.*, 32, Art. No. L09303.
- Delmelle, P., Delfosse, T., and B. Delvaux, (2003), Sulfate, chloride and fluoride retention in Andosols exposed to volcanic acid emissions, *Environmental Pollution*, 126, 445-457.
- Fayt, C. and M. van Roozendael (2001), WinDOAS 2.1—Software User Manual Belgisch Instituut voor Ruimte-Aeronomie Institut d'Aéronomie Spatiale de Belgique, Brussels, Belgium.
- Fickert, S., J.W. Adams, and J.N. Crowley (1999), Activation of Br₂ and BrCl via uptake of HOBr onto aqueous salt solutions, *J. Geophys. Res.* 104, 23719-23727.

- Finlayson-Pitts, B. J., M. J. Ezell, and J. N. Pitts (1989), Formation of chemically active chlorine compounds by reactions of atmospheric NaCl particles with gaseous N_2O_5 and ClONO_2 , *Nature*, 337, 241-244.
- Fish, D.J., and R. L. Jones (1995), Rotational Raman scattering and the Ring effect in zenith-sky spectra, *Geophys. Res. Lett.*, 22, 811-814.
- Francis P., Maciejewski A., Oppenheimer C., Chaffin C., and T. Caltabiano (1995), SO_2 :HCl ratios in the plumes from Mt. Etna and Vulcano determined by Fourier transform spectroscopy, *Geophys. Res Lett.*, 22, 1717-1720.
- Francis, P., M. R. Burton, and C. Oppenheimer (1998), Remote measurements of volcanic gas composition by solar occultation spectroscopy, *Nature*, 396, 567-570.
- Gerlach, T. M., and B. E. Nordlie (1975), The C-O-H-S gaseous system, part II: Temperaturw, atomic composition, and molecular equilibria in volcanic gases, *Am. J. Sci.*, 275, 377-394.
- Gerlach, T. M. (2004), Volcanic sources of tropospheric ozone-depleting trace gases, *Geochem. Geophys. Geosyst.*, 5, Q09007, doi:10.1029/2004GC000747.
- Lee, C., H. Tanimoto, N. Bobrowski, U. Platt, T. Mori, K. Yamamoto, and Y. J. Kim (2005), Detection of halogen oxides in a volcanic plume and observation of surface ozone depletion. *Geophys. Res. Lett.*, 32, L21809, doi:10.1029/2005GL023785.
- Lohberger, F., Hönninger, G., and U. Platt (2004), Ground based Imaging Differential Optical Absorption Spectroscopy of atmospheric gases, *Appl. Opt*, 43, (24), 4711-4717.
- Louban I. (2005), Zweidimensionale Spektroskopische Aufnahmen von Spurenstoff-Verteilungen, *Diploma Thesis*, University of Heidelberg (in German)
- Lowe, G. (2004), PocketDOAS Manuel, University of Heidelberg.

- Martin, R.S., T.A. Mather, and D.M. Pyle (2006), High-temperature mixtures of magmatic and atmospheric gases, *Geochem. Geophys. Geosys.*, 7, doi:10.1029/2005GC001186.
- Mather, T.A., D.M. Pyle, and C. Oppenheimer (2003), Tropospheric volcanic aerosol, in *Volcanism and the earth's atmosphere*, edited by A. Robock and C. Oppenheimer, *Geophysical Monograph 139*, American Geophysical Union.
- McGonigle, A., P. Delmelle, C. Oppenheimer, V. I. Tsanev, T. Delfosse, H. Horton, G. Williams-Jones, and T.A. Mather (2004), SO₂ depletion in tropospheric volcanic plumes, *Geophys. Res. Lett.*, 31, L13201, doi:10.1029/2004GL019990.
- Mellor, G. L., and T. Yamada (1982), Development of a Turbulence Closure Model for Geophysical Fluid Problems, *Rev. Geoph. Space Ph.*, 20, 851-875.
- Moreno, H., J. Clavero, and L. Lara (2004), Actividad explosiva post-glacial del Volcan Villarica, Andes del Sur. Septimo Congreso Geologico Cileno, Universidad de Concepcion, Concepcion, Chile, 329-333.
- Oppenheimer, C., Pyle, D.M., and Barclay, J. (editors), (2003) *Volcanic Degassing*, Geological Society, London, Special Publication, 213, 420pp.
- Oppenheimer, C., V. I. Tsanev, C. F. Braban, R. A. Cox, J. W. Adams, A. Aiuppa, N. Bobrowski, P. Delmelle, J. Barclay, and A. J. McGonigle (2006), BrO formation in volcanic plumes., *Geochimica et Cosmochimica Acta*, doi:10.1016/j.gca.2006.04.001, in press.
- Platt, U. and E. Lehrer (1997), Arctic Tropospheric Ozone Chemistry, ARCTOC, Final Report of the EU-Project No. EV5V-CT93-0318, Heidelberg
- Platt, U. and G. Hönninger (2003), The role of halogen species in the troposphere, *Chemosphere*, 52, 325–338.
- Robock, A. (2000), Volcanic Eruptions and Climate, *A. Reviews of Geophysics*, 38, 191-219.

- Sander, S. P., R. R. Friedl, D. M. Golden, M. J. Kurylo, R. E. Huie, V. L. Orkin, G. K. Moortgat, A. R. Ravishankara, C. E. Kolb, M. J. Molina, and B. J. Finlayson-Pitts (2003), Chemical Kinetics and Photochemical Data for Use in Stratospheric Modeling, *JPL Publication 02-25*, Jet Propulsion Laboratory, Pasadena, CA
- Seinfeld, J. H., and S. N. Pandis (1998), Atmospheric Chemistry and Physics, John Wiley & Sons, New York
- Stutz, J., and U. Platt (1996), Numerical Analysis and Estimation of the Statistical Error of Differential Optical Absorption Spectroscopy Measurements with Least-Squares methods, *Appl. Opt.*, 35, (30), 6041-6053
- Symonds, R.B., Rose, W.I., Bluth, G., and Gerlach, T.M. (1994), Volcanic gas studies: methods, results, and applications, in Carroll, M.R., and Holloway, J.R., eds., Volatiles in Magmas: Mineralogical Society of America Reviews in Mineralogy, v. 30, p. 1-66.
- Vié Le Sage, R. (1983), Chemistry of the volcanic aerosols, In Forecasting volcanic events, edited by H. Tazieff and J.C. Sabroux, pp. 445-474, Elsevier, Amsterdam.
- von Glasow, R., R. Sander, A. Bott, and P. J. Crutzen (2002), Modeling halogen chemistry in the marine boundary layer. 1. Cloud-free MBL. *J. Geophys. Res.*, 107D, (4341), doi:10.1029/2001JD000942.
- von Glasow, R., and P. J. Crutzen (2003), Tropospheric halogen chemistry, in: The Atmosphere (ed. R. F. Keeling), Vol. 4 Treatise on Geochemistry (eds. H. D. Holland and K. K. Turekian), 21 - 64, Elsevier-Pergamon, Oxford.
- von Glasow, R., and P. J. Crutzen, (2004), Model study of multiphase DMS oxidation with a focus on halogens, *Atmospheric Chemistry and Physics*, 4, 589 – 608.
- Watson, I. M., and C. Oppenheimer (2000), Particle size distributions of Mount Etna's aerosol plume constrained by Sun photometry, *J. Geophys. Res.*, 105, 9823 – 9829.

Wennberg, P. (1999), Bromine explosion, *Nature*, 397, 299-300.

Witter, J.B., V.C. Kress, P. Delmelle, and J. Stix (2004), Volatile degassing, petrology and magma dynamics of the Villarica Lava Lake, southern Chile, *J. Volcanol. Geotherm. Res.*, 134, 303-337.

Yvon, S., and H. Butler (1996), An improved estimate of the oceanic lifetime of atmospheric CH₃Br, *Geophys. Res. Lett.*, 23, 53-56.

Table 1

Initial composition of the gas phase compounds for the model runs in mixing ratio (mole mole⁻¹). See text for explanation of the four different cases.

Figure Captions:

Figure 1

(a) Map of the Mt. Etna volcano and its surroundings. The measurement sites of 2004 are marked by red dots, the measurement point of 2005 by red triangles.

(b) Map of the Villarica volcano and surroundings, the red dot shows the measurement site on November 17, 2004 and November 24, 2004, the blue arrow indicates the wind direction on the November 17, 2004.

Figure 2

One example of a plume scan for each distance (crater rim (several tenth of km from the vent) – (a) 100s of metres (“0 km”), (b) 1.5km, (c) 3km, (d) 6km, (e) 19km) measured at Mt. Etna in 2004. The slant column densities of BrO (blue – left y-axis) and SO₂ (red – right y-axis) are plotted versus the telescope elevation angle of the telescope.

Figure 3

One example of a scan for the Villarica plume at the summit (a) and 3 km further downwind (b). The slant column densities of BrO (blue) and SO₂ (red) are plotted versus the telescope elevation angle of the telescope.

Figure 4

The BrO/SO₂ ratios for the different measurements at distances up to 19 km from the summit. The autumn 2004 data from Mt. Etna is shown as red dotted bars (average value over three days or more measurement days on the specific locations except for the data close to the source and at 19km distance which only contain few data points from only one day) and 2005 data as red solid bars. The 2004 Villarica data is displayed in solid blue bars.

Figure 5

Vertical profile of the BrO/SO₂ ratio as a vertical profile of the plume was calculated from the two-dimensional BrO and SO₂ distributions measured by the Imaging DOAS instrument. The measurements were taken at a distance of about 10 km downwind of the crater region on the eastern flank of Mt. Etna on the May 10, 2005 between 2:00 pm and 2:30 pm. The highest BrO/SO₂ values are found at the edges of the plume, which is additionally indicated by the solid line. R on the right panel shows the correlation coefficient for every single calculated BrO/SO₂ ratio.

Figure 6.1

Location of the measurement on October 1, 2004 (red triangle) and of different craters (NE - Northeast crater, SE - Southeast crater, BN - Bocca Nova, VOR – Voragine). The grey shading indicates the volcanic gas emission (plumes of the different craters).

Figure 6.2

One example of a plume scan of Mt. Etna October 1, 2004. Measurements were carried out at a height of 2900 m on the southern side of Mt. Etna. The slant column densities of BrO (blue) and SO₂ (red) are plotted over the telescope elevation angle of the telescope. Two plumes with different BrO/SO₂ ratios are observed, for further explanation see text.

Figure 7.1

The calculated BrO/SO₂ ratio for all measurements carried out at Rifugio Citelli, situated about 6 km downwind on the eastern flank of Mt. Etna (see Figure 1 point d). Temporal variations are visible on short and ‘longer’ timescale. A general trend shows an increased scatter in the BrO/SO₂ value in 2005, which can be explained by the scatter in wind directions (see text).

Figure 7.2

Wind directions for October 10 – 18, 2004 and May 5 – 19, 2005.

Figure 8

One example of a plume scan of Mt. Etna August 5, 2004. Measurements were carried out at Pizzi Deneri scanning the plume 3 km downwind of the summit (see Figure 1, point c). The slant column densities of BrO (blue circles), SO₂ (red triangles), ClO (cyan diamond), OCIO (dark yellow square) are plotted over the telescope elevation angle.

Figure 9

Spectral fit result for one example of OCIO detection. The fit was done with WinDoas V2.10 from IASB (Belgium Institute for Space Aeronomy, [Fayt and Van Roozendael, 2001]) in the spectral range of 362 – 390 nm. The left panel shows the OCIO absorption bands in red, the measured spectrum in black. The right panel shows the residual for this fit, with a peak to peak optical density of 1.5 %. The spectra was taken on the 5th of August at noon at an telescope elevation angle of 35 °.

Figure 10

Model simulation: Contour plots of the vertical and temporal evolution of model run “60-40”. Shown are the mixing ratios in mol mol⁻¹ for the main compounds and the molar ratio of BrO/SO₂. Time is in minutes since model start and altitude in m. The plume is emitted 11 minutes after model start at an altitude of 3340 m. The spatial extent of plume can best be seen from log(SO₂).

Figure 11a:

Temporal evolution of the first 80 minutes after model start of the calculated vertical columns (in molecules/cm²) for the measured species. The colour code is as follows: case “60-40” – black, solid line, “85-15” – ‘red’, dashed line, “pure” ‘green’, dash-dotted line, “arc mean” ‘blue’, dotted line (see text for an explanation of the different scenarios). As the vertical columns of ClO differ strongly between the model scenarios, the ClO VCD is plotted twice with different scaling in order to show both the differences between the runs and the maximum numbers for run "60-40". In the model the plume is emitted after 11 minutes as marked by the vertical red lines, the measurements cover roughly the first 30-60 minutes after plume release. The approximate range of the measurements for the BrO/SO₂ ratio is indicated by the shaded region, where the distance from the crater has been converted to time since emission assuming a wind speed of about 7 m s⁻¹.

Figure 11b

Same as Figure 11a for BrO vertical column and the ratio BrO/SO₂ but shown until the end of the model runs to highlight that the BrO/SO₂ ratio continues to rise downwind of the crater (showing a maximum more than two hours after plume release) even though the BrO vertical column decreases strongly.

Figure 12

Sketch of processes in a volcanic plume: after emission of volcanic gases, that mix with ambient air and thus forming a plume; ozone becomes available and radical chemistry starts. As a consequence the initial hydrogen halides are heterogeneously converted to halogen oxides. See text for more details.

	„60:40“	„85:15“	pure	arc mean
NO	2.7500e-06	2.5704e-05	1.2600e-11	1.9950e-05
NO ₂	2.5700e-07	1.9050e-07	1.5800e-14	1.0000e-07
SO ₂	3.7200e-03	2.0890e-02	2.6000e-02	1.5800e-02
H ₂ SO ₄	7.7600e-05	3.8900e-07	7.2400e-13	6.3100e-07
O ₃	1.5800e-14	0	0	0
H ₂ O ₂	3.1623e-11	1.2300e-09	3.1600e-13	1.7780e-09
HCl	7.7630e-03	1.0965e-02	1.2880e-02	6.3100e-03
HOCl	2.7500e-07	4.4670e-07	3.9800e-12	2.2400e-07
Cl ₂	3.4670e-05	4.0740e-06	6.3100e-12	1.0000e-06
HBr	8.5100e-06	3.8900e-05	6.3360e-03	1.0000e-05
HOBr	8.9000e-08	1.9500e-08	7.0000e-08	2.8200e-08
Br ₂	2.7540e-06	1.7780e-07	1.3900e-07	1.2590e-08
BrCl	2.2390e-05	1.8620e-06	2.1500e-06	2.5120e-07
CO	7.9000e-14	3.7150e-09	1.1200e-09	3.7000e-09
SO ₃	1.1700e-02	1.2300e-03	8.5000e-11	1.0000e-03
CO ₂	5.2500e-02	7.4000e-02	4.6000e-02	4.6000e-02
OH	1.1500e-08	3.3110e-06	1.3500e-10	3.1620e-06
HO ₂	4.0740e-10	1.7780e-08	2.5200e-13	6.3100e-09
Cl	2.5120e-07	6.6070e-06	1.1700e-10	2.5120e-06
ClO	6.9180e-09	5.2480e-08	3.1600e-13	1.5850e-08
Br	1.6600e-06	1.3200e-05	5.3700e-04	3.1620e-06
BrO	5.2480e-01	4.1690e-09	6.2300e-09	6.3096e-10
H ₂ O	4.6770e-01	6.6370e-01	9.1900e-01	9.1900e-01